

RESEARCH ARTICLE



OPEN ACCESS

Received: 16-12-2023

Accepted: 10-05-2024

Published: 29-05-2024

Citation: Damor AB, Patel VJ (2024) Response Surface Optimization for Compliant Joint of Humanoid Robot Using ANSYS - Design of Experiment. Indian Journal of Science and Technology 17(22): 2271-2282. <https://doi.org/10.17485/IJST/v17i22.3169>

* **Corresponding author.**

alpeshtdamor@gmail.com

Funding: None

Competing Interests: None

Copyright: © 2024 Damor & Patel. This is an open access article distributed under the terms of the [Creative Commons Attribution License](https://creativecommons.org/licenses/by/4.0/), which permits unrestricted use, distribution, and reproduction in any medium, provided the original author and source are credited.

Published By Indian Society for Education and Environment ([iSee](https://www.indjst.org/))

ISSN

Print: 0974-6846

Electronic: 0974-5645

Response Surface Optimization for Compliant Joint of Humanoid Robot Using ANSYS - Design of Experiment

Alpeshkumar B Damor^{1,2*}, Vinay J Patel³

¹ Ph.D. Research scholar, Gujarat Technological University, Gujarat, India

² Assistant professor, Mechanical Engineering Department, BVM Engineering College, Anand, Gujarat, India

³ Professor & Head of Department, Mechanical Engineering Department, BVM Engineering College, Anand, Gujarat, India

Abstract

Objective: A Compliant Joint of humanoid robot is a spring-loaded assembly, which is used to interact safely with the environment, and it helps to stabilized sudden shock and vibration in the robotic system. At the moment, compliant joints are required to optimize their size and dimensions which result into optimized weight and factor of safety of humanoid robot. **Methods:** Analysis is carried out using Response Surface Methodology (RSM) and Multi-Objective Genetic Algorithm (MOGA) using ANSYS. The current study employed goal-driven optimisation using ANSYS Workbench to minimise weight and achieve the required factor of safety range for the compliant joint. To find out range of variables such as rim thickness, shaft diameter, base thickness, module thickness and spoke thickness affecting on responses such as factor of safety and geometrical mass of compliant joint single factor single response parametric analysis is carried out. **Findings:** Based on trend of preliminary analysis variable range and combinations are selected to study interaction effect of parameters to obtain favorable factor of safety and low geometrical mass. The optimized compliant joint is compared with various design and validated through the developed actual module. **Novelty:** Eventually, the geometry mass of the compliant joint was reduced from 0.8604 kg to 0.6449 kg, resulting in a lighter weight (24.06% reduction) with a 1.7533 factor of safety and more compact in size (outer diameter is shrink from 142 to 126 mm).

Keywords: Compliant joint; Goal driven optimization; Response surface optimization; Design of experiment; Humanoid robot

1 Introduction

Whenever, a robot shares working space with humans and possibilities of robot-human interactions, safety of humans is the most important issue to address. Human body joint has attractive characteristics – “Compliance”. Due to compliance in joints, a human can crash an aluminium and at same time able to pick very soft object like flower. It is also

able to perform very stiff and accurate motions or moving softly to reduce possible injuries in case of unexpected collisions. Moreover, it permits to store energy and release it quickly, for example, throwing an object or jumping, etc. compliance in robot joints will increase safety of humans whenever there is robot-human interactions.

Many researchers have studied these characteristics deeply and develop robotic joints with compliance (compliant joint). Compliant joints of robot are contributing an important role to ensure safety of humans⁽¹⁾. The compliant robotic joints can be categorized in three categories: 1) Passive 2) Active and 3) Variable Impedance Actuator (VIA). Passive elements (springs) in passive compliant joint, are arranged into the joint to improve safety but joint performance is largely affected. Active compliance obtained by controlling rigid joints such as to emulate compliant behaviour. The principal disadvantage of this approach is that energy cannot be stored, and some safety issue cannot be completely solved. Variable Impedance Actuator (VIA) actively controls passive compliance. VIA characterized in such a way that passive elements inside the device can be controlled in order to vary the joint compliance. This approach looks to be the best thread-off between safety, capabilities and performance⁽²⁾.

Series Elastic Actuator (SEA), a type of Variable Impedance Actuator (VIA), is an actuator which receives much attention as the next-generation actuator⁽³⁾. Since it was first introduced in 1995, SEA has been currently recognized in the robotics field as an actuator system to implement a high-performance torque control⁽⁴⁾⁽⁵⁾. A SEA is comprising of motor, spring, gear and load. With different kind of arrangements of these elements various types and configuration of mechanism have been developed as SEAs to satisfy many requirements necessary for the applications. SEAs are categorised into Force-sensing SEA, Reaction Force-sensing SEA and Transmitted Force-sensing SEA based on the relative location of the spring⁽⁶⁾.

Couple of baby humanoid robots have developed using certain joints as compliant joints: cCub (Biped)⁽⁷⁾⁽⁸⁾ and COMAN⁽⁹⁾⁽¹⁰⁾. These developments have shown excellent stability control and other performance with compliant joints. However, they are not full-sized humanoid robots. Moreover, few of joints are not compliant joints due to complexity and space requirements. A full-sized humanoid will require more energy to be stored and better stability control. An optimised design of compliant joint will help to develop full-sized humanoid robot with compliant joints.

For 2-DOF (Ankle joint) and 3-DOF (Thai joint) for full-sized humanoid robot, it cannot be directly used because it is large in size and heavy in weight. Therefore, it is required a new arrangement for the more DOF or need to optimize compliant joint for small in size and light in weight. Parametric optimization techniques, which is used to help designers determine the optimal shape and dimensions of a structure. By using black box model, the different optimization techniques like a DOE, Response surface, Goal driven can be implemented using ANSYS are explained in⁽¹¹⁾. The response surface optimization can be performed in ANSYS using the Design of experiments, Response surfaces, and objective and constrains. Before the DOE, parameter selection and range of parameter selection is main criteria to perform optimization process. In DOE, the suitable method needs to be selected for DOE table preparation. Response surface methodology and finite element analysis with particle swarm optimization (PSO) algorithm result accurate optimization for Compliant Rotary Joint⁽¹²⁾. Further, response surfaces can be generated which shows the sensitivities from graphs using the available methods. As per the objective and constrains decided by authors, the best candidate point is generated at the end of the MOGA⁽¹³⁾⁽¹⁴⁾.

This paper explains design of compliant joints used in humanoid robot and its optimization process. The response surface method, the design of the experiment, and multi-objective genetic optimization with ANSYS are used to obtain an optimised design of a compliant joint of a humanoid robot.

2 Methodology

2.1 Design of Compliant Joint and its Fea

2.1.1 Three spoke compact SEA design

A compact series elastic actuator (SEA) for small humanoid is presented in⁽⁷⁾. This novel and compact design suggests three spoke spring coupling arrangements. A compliant joint to transmit maximum 120 N-m torque (requires for leg joints of full-sized humanoid) is designed based on this suggested design. The outer circular disk used as the input of the compliant joint and is connected to the output of the reduction drive preferably harmonic drive. The three spoke element rotates on bearings with respect to the circular base and is coupled with it by means of six springs as shown in Figure 1. The three spoke component forms the output of the compliant joint and the mounting base of the output link. The six linear springs when inserted in the arrangement shown in Figure 1 experience a pre-contraction equal to half of the maximum acceptable deflection.

2.1.2 FEA of suggested design

Finite element analysis (FEA) is performed to evaluate the strength of the suggested compliant joint for full-sized humanoid under the maximum load conditions. Static structural module of ANSYS Workbench is used for the FEA. The CAD model is

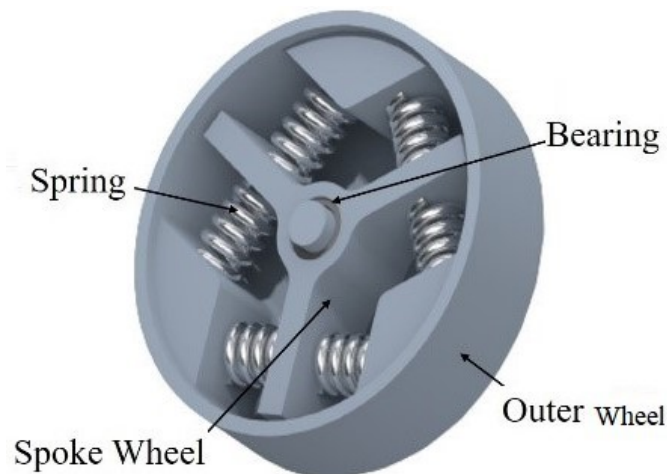


Fig 1. CAD Model of compliant joint

developed in CREO 5.0 and is directly imported into ANSYS workbench 2020 R2 with no data loss. Aluminium 6061-T6 is considered as the material for outer wheel and spoke wheel as it has better weight-to-strength ratio and good machinability properties. The material properties considered in the analysis is shown in Table 1.

Table 1. Material Properties of components of the compliant joint

Sr. No.	Young's Modulus (GPa)	Poisson's ratio	Yield Strength (MPa)	Tensile Strength (MPa)
1	68.9	0.33	276	310

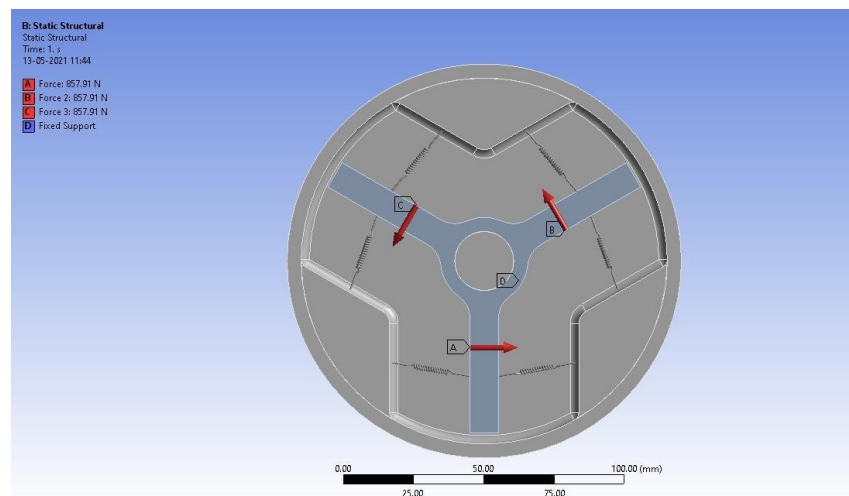


Fig 2. External force applied on each Spoke

A compliant joint assembly has two parts as spoke wheel and outer wheel as shown in Figure 1. This connection between spoke wheel and outer wheel is considered as frictionless contact and revolute joint for the FEA analysis. ANSYS software provide a facility to select spring element and work as an actual spring by taking data of spring stiffness, preload, free length and material from users. A model is designed for 120 Nm torque capacity. For that, externally force is applied on spoke wheel, which is divided by three spokes and applied individually in same direction as shown in Figure 2. Six holes on the outer wheel which are used to mount compliant joint on reduction gear (harmonic drive) are constrained. Meshing is done individually for all the parts of assembly using multi-zone methods. Quadrilateral and tetrahedron meshing types are created and further

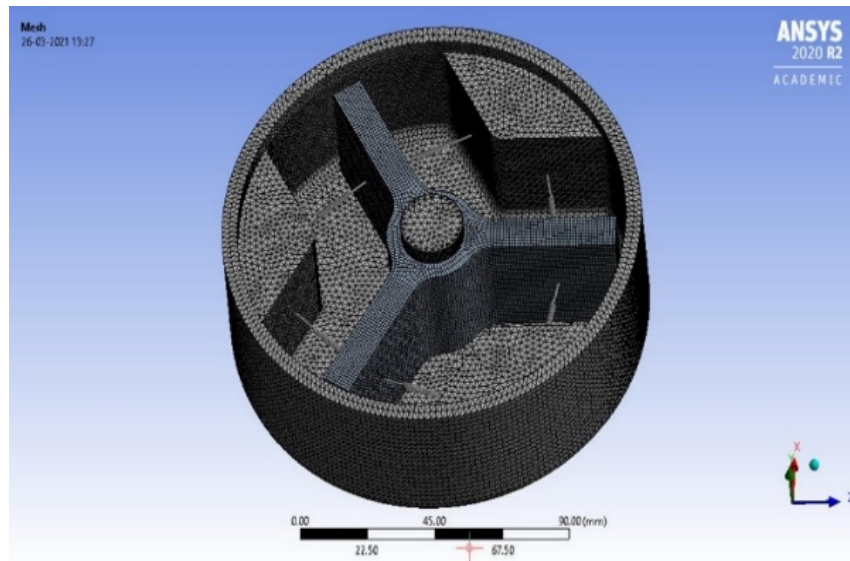


Fig 3. Meshing of each component of compliant joint

refinements is done using face and size meshing methods to improve the mesh quality. The average value of element quality is nearer to one, which indicates the best quality of mesh shown in Figure 3. The FEA results factor of safety equals to 3.54. The total weight of compliant joint is 0.8604 kg. Von-Mises stresses are shown in Figure 4. The maximum Von-Mises stress is 89.798 MPa.

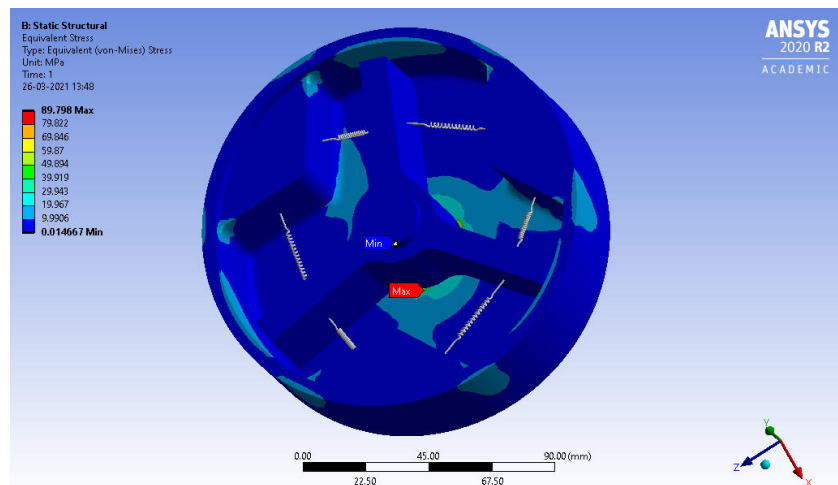


Fig 4. Von-Mises Stress in compliant joint

2.2 Optimization of Compliant Joint

2.2.1 Sensitivity Analysis for parameter selection

The optimization process shall be start with the selection of design variables (parameters). For the selection of design variable, sensitive analysis is performed in ANSYS to understand effect of variation in individual key parameters on total weight of compliant joint and factor of safety. The selected parameters for analysis are shaft diameter, base thickness, module thickness, spoke thickness, rim thickness, spoke length and pitch circle diameter as shown in Figure 5. Rest of the dimensions of the compliant joint have parametric relation/s with these parameters. Sensitivity analysis suggests that out of these seven parameters,

five parameters are sensible for total weight of compliant joint and factor of safety.

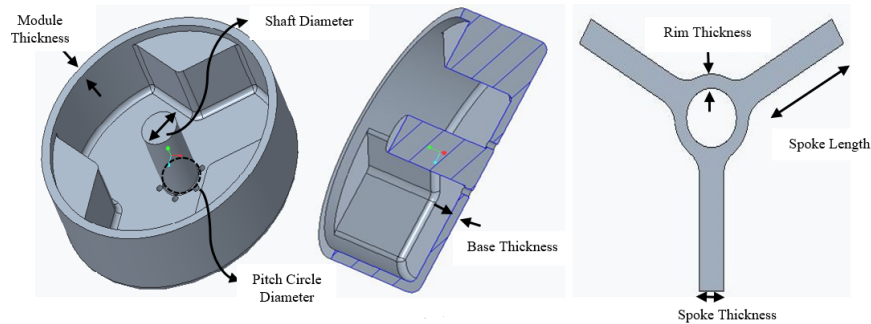


Fig 5. Selected design variables

After sensitivity analysis, a response graph is plotted, which helps to select the range of parameters as well as find non-significant parameters that can be made constant during further detailed analysis. Two graphs for each parameter shows the comparison between geometry mass vs. parameter range and factor of safety vs. parameter range, respectively.

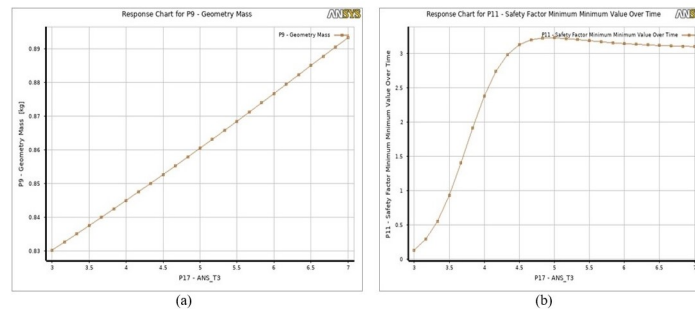


Fig 6. Response analysis for Rim thickness for variation of 3 to 7 mm

Figure 6(a) and (b) show the response graphs for rim thickness in the range of 3 to 7 mm. Graphs depict that as the rim thickness reduces, the geometry mass reduces. For the same range, the value of the factor of safety decreases with a decrease in rim thickness. Therefore, spoke length can be fixed from the graphs. The graph shows that at the rim thickness of 4 mm, the factor of safety is 2.4, which is well between our selected ranges of 3 and 7 mm.

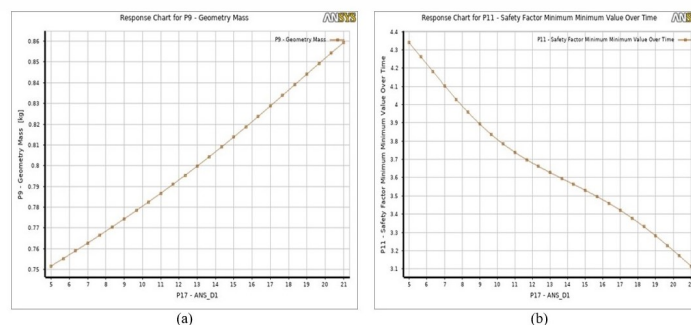


Fig 7. Response analysis for shaft diameter for variation of 5 to 21 mm

Figure 7(a) and (b) show response graphs for shaft diameter in the range of 5 to 21 mm. Graphs depict that as the shaft diameter reduces, the geometry mass reduces. For the same range, the value of the factor of safety increases with a decrease in shaft diameter. The shaft with bearing will work as a locator for the spoke wheel. The minimum shaft diameter with bearing can

be accepted as 12 mm (on an 8 mm shaft, HK 0812 RS bearing mounted). From the graphs, the shaft diameter is selected as a design variable to further proceed to check the combined effects of all selected parameters.

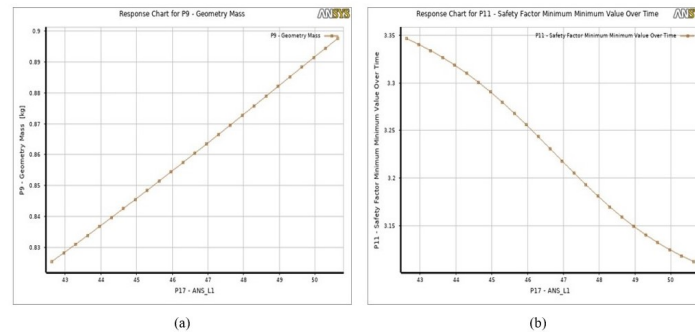


Fig 8. Response analysis for Spoke length for variation of 43 to 50 mm

Figure 8(a) and (b) show response graphs for spoke length in the range of 43 to 50 mm. Graphs depict that as the spoke length reduces, geometry mass reduces. For the same range, the value of Factor of Safety increases with a decrease in spoke length. In between every block and spoke, a spring is placed for design perspective. Moreover, it requires a gap size 30 mm in between them. Therefore, the spoke length should not be less than the existing dimensions. It is selected as a fixed target in objectives.

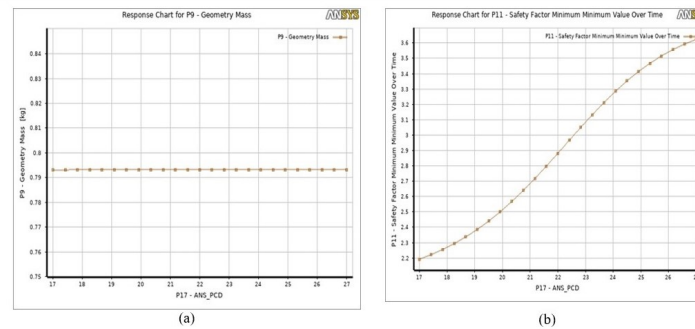


Fig 9. Response analysis for Pitch Circle Diameter for variation of 17 to 27 mm

Figure 9(a) and (b) show response graph analysis for pitch circle diameter in the range of 17 to 27 mm. Graphs depict that as the pitch circle diameter reduces, geometry mass remains constant. However, pitch circle diameter changes with shaft diameter, and shaft diameter is selected as a design variable. Therefore, this parameter is considered as a design variable.

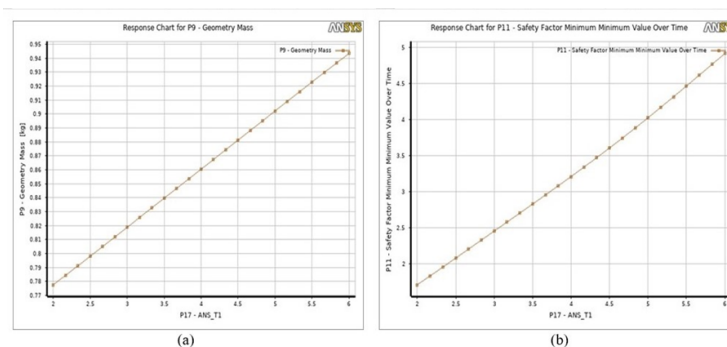


Fig 10. Response analysis for Base Thickness for variation of 2 to 6 mm

Figure 10(a) and (b) show response graph analysis in the range of 2 to 6 mm. Individual single factorial design analysis indicates that the base thickness of the compliant joint module has a linear relationship with factors of safety and geometric mass.

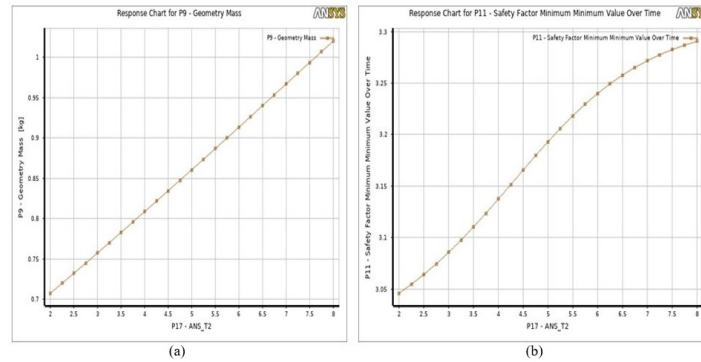


Fig 11. Response analysis for Module Thickness for variation of 2 to 8 mm

Figure 11(a) and (b) shows response graphs analysis in range of response 2 to 8 mm variation. Individual single factorial design analysis indicates that module thickness of compliance joint module have linear relation with factor of safety and geometric mass.

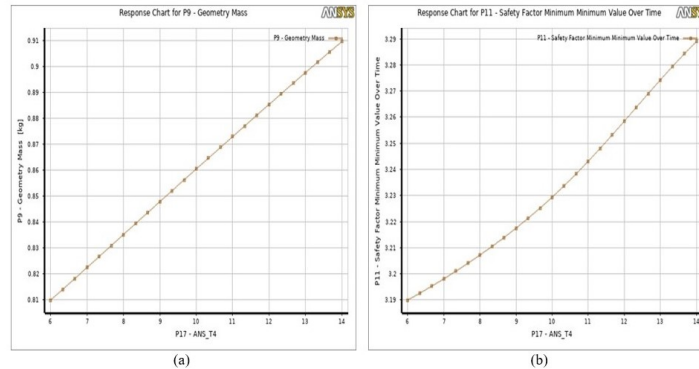


Fig 12. Response analysis for Spoke Thickness for variation of 6 to 14 mm

Figure 12(a) and (b) shows response graph analysis of 6 to 14 mm for spoke thickness variation. The response of the graph indicates that as the parameter value reduces geometry mass reduces and Factor of Safety decreases. It is always difficult to find effect of multiple factors at one time on single response variable or multi response variable. Hence, for optimum compliance design factor of safety and weight possess equal weightage. Table 2 shows initial value of the parameter and its range suggested by sensitivity analysis.

Table 2. Selected design variables and Suggested range

Design variables	Initial Value (mm)	Suggested Range (mm)
Shaft Diameter	21	12 to 21
Spoke Length	46.63	42.63 to 50.63
Base Thickness	4	2 to 6
Module Thickness	5	2 to 8
Spoke Thickness	10	6 to 14

2.2.2 Design of Experiment for compliant joint

It is important to perform design of experiment and multi criteria decision-making to find interaction (combine) effect of compliant joint variables on Factor of safety and weight. Response surface design and goal driven optimization is one of the best solution, which helps to reduce possible interaction for performing the analysis. The design of experiments helps to calculate the responses values for specifically defined upper and lower values of design variable. It is a time saving and low-cost activity^{(12) (13)}. With combination of response surface modelling, to effectively map out a parametric design space using DOE helps to perform minimum number of design combinations which saves resource and time. The face-centered method from Central Composite Design Model (CCD) is performed for DoE which has three levels to divide the various modes of input parameters. Therefore, each input parameter is divided into three levels between its maximum and minimum values. Hence, total 27 sample points (experiments) are generated for five parameters. Table 3 shows all 27 experiments with resulted total mass of compliant joint and factor of safety.

Table 3. Response Surface design for compliant joint

Expt. No.	Shaft Diameter (mm)	Spoke length (mm)	Base Thickness (mm)	Module Thickness (mm)	Spoke Thickness (mm)	Mass (kg)	Safety Factor Minimum
1	16.5	46.63	4	5	9	0.798	0.483
2	12	46.63	4	5	9	0.768	0.255
3	21	46.63	4	5	9	0.832	3.170
4	16.5	42.63	4	5	9	0.766	0.479
5	16.5	50.63	4	5	9	0.833	0.466
6	16.5	46.63	2.5	5	9	0.741	0.288
7	16.5	46.63	5.5	5	9	0.855	0.477
8	16.5	46.63	4	2.5	9	0.676	0.476
9	16.5	46.63	4	7.5	9	0.925	0.470
10	16.5	46.63	4	5	6	0.760	2.622
11	16.5	46.63	4	5	12	0.835	2.712
12	12	42.63	2.5	2.5	12	0.617	1.517
13	21	42.63	2.5	2.5	6	0.595	0.568
14	12	50.63	2.5	2.5	6	0.579	1.259
15	21	50.63	2.5	2.5	12	0.711	1.883
16	12	42.63	5.5	2.5	6	0.635	3.015
17	21	42.63	5.5	2.5	12	0.763	4.019
18	12	50.63	5.5	2.5	12	0.771	2.854
19	21	50.63	5.5	2.5	6	0.755	0.545
20	12	42.63	2.5	7.5	6	0.768	1.348
21	21	42.63	2.5	7.5	12	0.898	2.103
22	12	50.63	2.5	7.5	12	0.907	1.347
23	21	50.63	2.5	7.5	6	0.892	0.539
24	12	42.63	5.5	7.5	12	0.936	3.224
25	21	42.63	5.5	7.5	6	0.946	0.571
26	12	50.63	5.5	7.5	6	0.955	2.668
27	21	50.63	5.5	7.5	12	1.120	4.2322

2.2.3 Response Surfaces of parameters

A response surface is generated from the DOE results for each output parameter. It gives the sensitivities of the output parameters (responses) concerning to the input parameters⁽¹⁵⁾. It has been observed that combined effect of shaft diameter and base thickness (Figure 13) and shaft diameter and module thickness (Figure 14) has shown non-linear relationship which are shown in Figure 13 and Figure 14 respectively.

2.2.4 Objective and Constraints

Ultimately, the optimisation problem is stated as follows, and to obtain an optimised design, the Multi-objective Genetic Algorithm with ANSYS is employed.

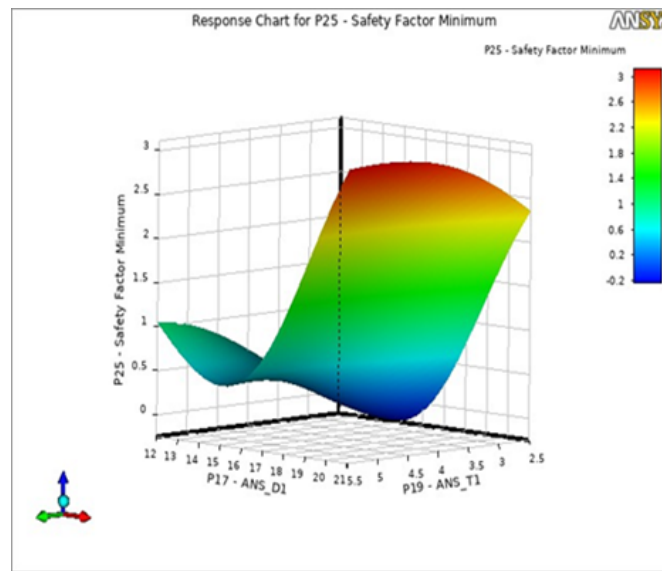


Fig 13. Response Surface for Safety factor vs. Shaft diameter (P17) and Base thickness (P19)

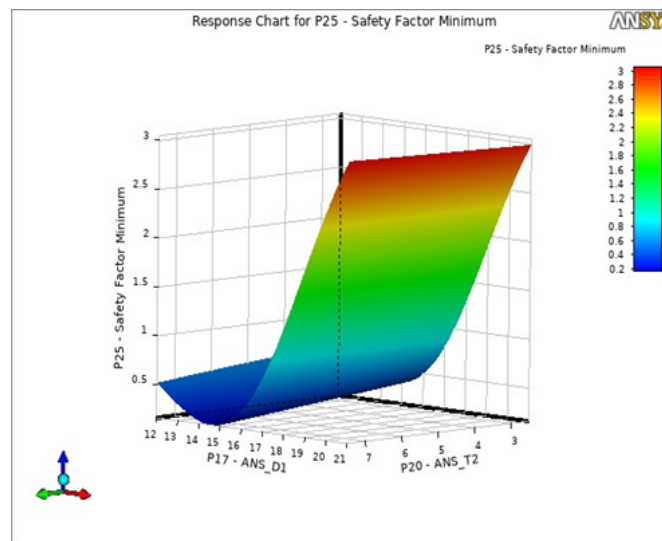


Fig 14. Response Surface for Safety factor vs. Shaft diameter (P17) and Module thickness (P20)

Table 4.

Objectives	Constraints
1. Minimize [Total mass of compliant Joint]	1. Shaft diameter: 12 to 21 mm
2. Factor of Safety [Between 1.5 to 2.5]	2. Spoke length: 46.63 mm
	3. Base thickness: 2 to 6 mm
	4. Module thickness: 3 to 8 mm
	5. Spoke thickness: 6 to 14 mm

3 Result and Discussion

The Trade-off chart shows feasible and infeasible points for Geometry mass vs. factor of safety in Figure 15. The best set of samples is indicated in blue. The worst set of samples is indicated in red. The best candidate point is selected from these samples.

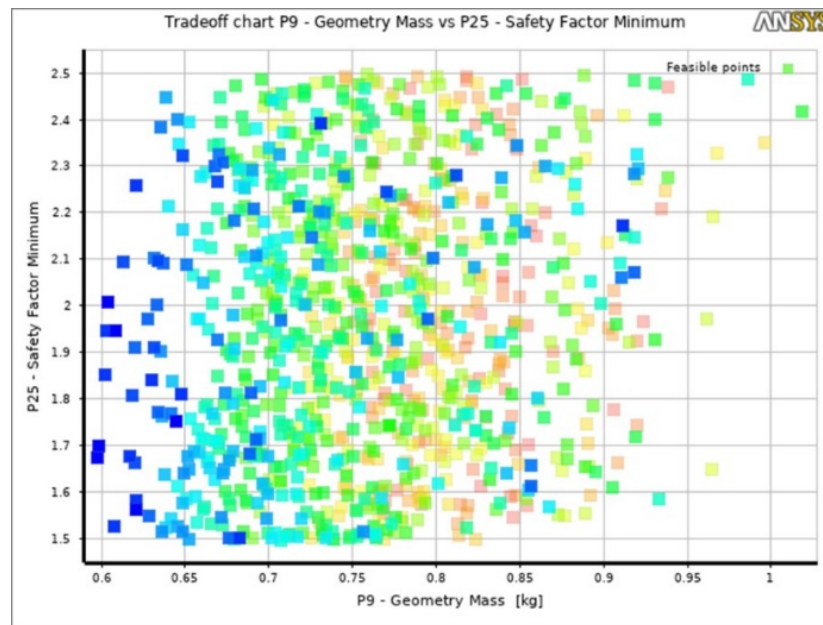


Fig 15. Trade off Chart: Geometry mass vs. Factor of safety

The Overall sensitivity chart shown in Figure 16 indicates the combined effects of all the selected parameters to the output parameters. Rim thickness and pitch circle diameter have negligible effect hence they are discarded in further study. The module thickness is highly sensitive for geometry mass comparatively to other parameters. The shaft diameter and spoke lengths are highly sensitive for total deformation of model comparatively to other parameters. The shaft diameter, Spoke thickness and base thickness are sensitive for safe design comparatively to other parameters.

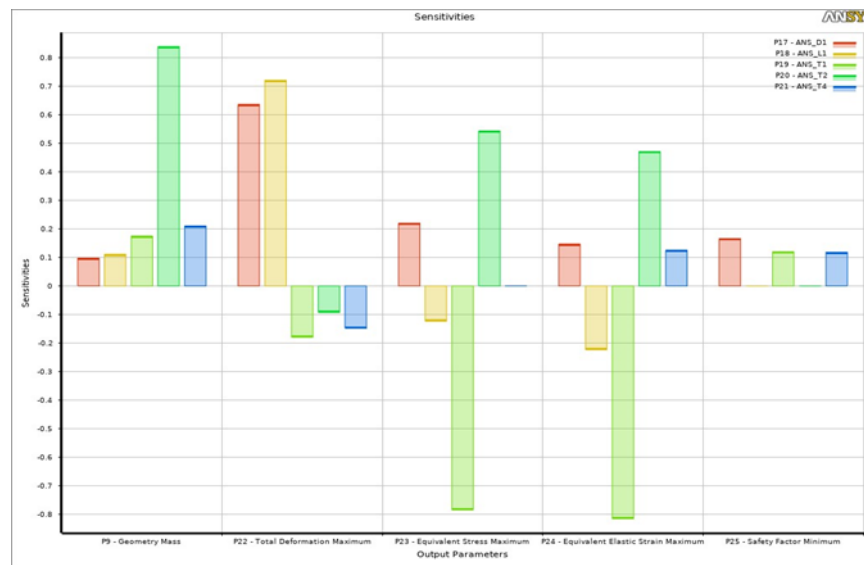


Fig 16. Overall sensitivity of parameters

After the optimization studies for set objectives and set constraints, results indicate that design variable shall be set to shaft diameter: 12.003 mm, shaft length: 46.33 mm, base thickness: 3.5005 mm, rim thickness: 4.00 mm, spoke thickness: 6.857 mm of compliant joint. The module gives best factor of safety 1.7533 and total weight of compliant joint 0.6449 kg.

3.1 Validation of Optimized Compliance Design

Parameters before and after optimization and parameters are rounded as per the acceptability are presented in Table 4. FEM analysis is carried out to show the effect of optimized design using static structural analysis⁽¹⁶⁾. Figure 17 shows the von mises stress distribution for optimized module by performing static structural analysis. It can be seen from the results that the mass of the previous module is 0.8604 kg, which is reduced to 0.6449 kg. It shows that after the optimization, 24.06 % weight is reduced. Outer diameter is shrieked from 142 to 126 mm which indicates compactness of optimized design. The factor of safety value is lies in between the acceptable range.

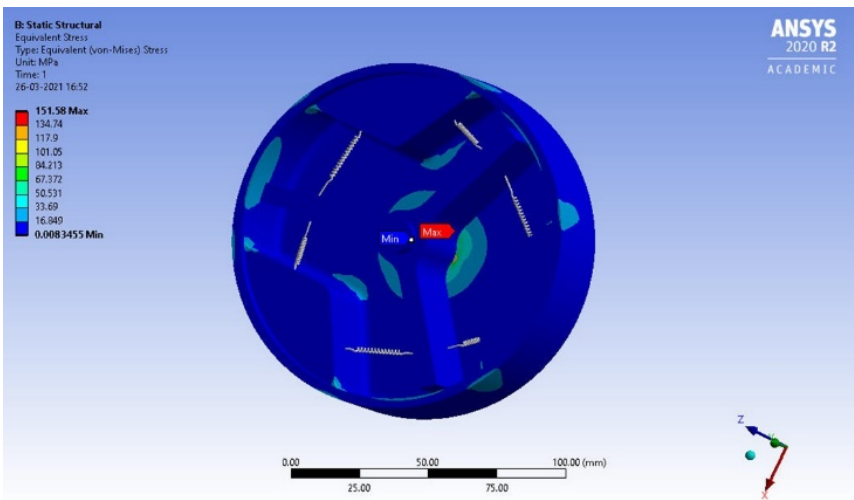


Fig 17. Von Mises stress distribution for optimized module

Table 5. Result comparison Initial and optimized

		Initial	Optimized	Rounded
Parameters (mm)	Shaft Diameter	21	12.003	12
	Shaft Length	46.63	46.63	46.63
	Base thickness	4	3.5003	3.5
	Module Thickness	5	3.5005	3.5
	Rim Thickness	5	4	4
	Spoke Thickness	10	6.8577	6.85
Response	Geometry Mass (kg)	0.8604	0.6449	0.6534
	Factor of Safety	3.2294	1.7533	1.9132

4 Conclusion

In this study, structural optimization and design of experiment methods were used in order to obtain an optimum and lighter design of compliant joint. After finite element analysis was conducted for initial design of the compliant joint, it has seen that compliant joint was over designed. The sensitivity analysis has suggested that rim thickness and pitch circle diameter have negligible effect hence they are discarded in the study. The sensitivity analysis has further suggested range of remaining parameters for design of experiments. 27 sample points (experiments) are generated for five parameters to observe their effect on responses (factor of safety and total weight of compliant joint). Then, response surfaces have been generated to evaluate combined effect of parameters. It has been observed that combined effect shaft diameter and base thickness (Figure 13), and shaft diameter and module thickness (Figure 14) has shown non-linear relationship. Finally, two objective functions and constraint (suggested by sensitivity analysis) are set for multi objective genetic algorithm (MOGA). The best candidate point

is selected from trade-off chart generated by MOGA. FEA of the best candidate point results that 24.06% weight of compliant joint is decreased with 1.7533 factor of safety. Outer diameter shrunk from 142 to 126 mm results into more compact design of humanoid robot.

Acknowledgement

The authors express their deep gratitude to the Mechanical Engineering Department at Birla Vishvakarma Mahavidyalaya and Gujarat Technological University (GTU) for the invaluable support in providing essential hardware and software resources, which significantly contributed to the success of this research.

References

- 1) Damme MV, Beyl P, Vanderborgh B, Ham RV, Vanderniepen I, Matthys A, et al. The role of compliance in robot safety. In: Proceedings of the Seventh IARP Workshop Seventh IARP Workshop on Technical Challenges for Dependable Robots in Human Environments. IARP + IEEE. 2010;p. 65–71. Available from: <https://researchportal.vub.be/en/publications/the-role-of-compliance-in-robot-safety>.
- 2) Flacco F. Modeling and Control of Robots with Compliant Actuation. Rome, Italy. 2012.
- 3) Vanderborcht B, Albu-Schaeffer A, Bicchi A, Burdet E, Caldwell DG, Carloni R, et al. Variable impedance actuators: A review. *Robotics and Autonomous Systems*. 2013;61(12):1601–1614. Available from: <https://dx.doi.org/10.1016/j.robot.2013.06.009>.
- 4) Williamson MM. Series Elastic Actuators. 1995. Available from: https://groups.csail.mit.edu/lbr/hrg/1995/mattw_ms_thesis.pdf.
- 5) Pratt GA, Williamson MM. Series elastic actuators. In: Proceedings of the 1995 IEEE/RSJ International Conference on Intelligent Robots and Systems. IEEE. 2002. Available from: <https://doi.org/10.1109/IROS.1995.525827>.
- 6) Lee C, Kwak S, Kwak J, Oh S. Generalization of Series Elastic Actuator Configurations and Dynamic Behavior Comparison. *Actuators*. 2017;6(3):1–26. Available from: <https://dx.doi.org/10.3390/act6030026>.
- 7) Tsagarakis NG, Lafranchi M, Vanderborcht B, Caldwell DG. A compact soft actuator unit for small scale human friendly robots. In: 2009 IEEE International Conference on Robotics and Automation. IEEE. 2009. Available from: <https://doi.org/10.1109/ROBOT.2009.5152496>.
- 8) Tsagarakis NG, Li Z, Saglia J, Caldwell DG. The design of the lower body of the compliant humanoid robot “cub”. In: 2011 IEEE International Conference on Robotics and Automation. IEEE. 2011. Available from: <https://doi.org/10.1109/ICRA.2011.5980130>.
- 9) Li Z, Vanderborcht B, Tsagarakis NG, Colasanto L, Caldwell DG. Stabilization for the compliant humanoid robot COMAN exploiting intrinsic and controlled compliance. In: 2012 IEEE International Conference on Robotics and Automation. IEEE. 2012. Available from: <https://doi.org/10.1109/ICRA.2012.6224705>.
- 10) Tsagarakis NG, Morfey S, Cerda GM, Zhibin L, Caldwell DG. COMpliant huMANoid COMAN: Optimal joint stiffness tuning for modal frequency control. In: 2013 IEEE International Conference on Robotics and Automation. IEEE. 2013. Available from: <https://doi.org/10.1109/ICRA.2013.6630645>.
- 11) Chen X, Liu Y. Finite Element Modeling and Simulation with ANSYS Workbench. 2nd ed. Boca Raton. CRC Press - Taylor and Francis Group. 2019. Available from: <https://doi.org/10.1201/9781351045872>.
- 12) Chau NL, Le HG, Dao TP, Dang MP, Van Anh Dang. Efficient Hybrid Method of FEA-Based RSM and PSO Algorithm for Multi-Objective Optimization Design for a Compliant Rotary Joint for Upper Limb Assistive Device. *Mathematical Problems in Engineering*. 2019;2019:1–14. Available from: <https://dx.doi.org/10.1155/2019/2587373>.
- 13) Chau NL, Le HG, Dao TP, Van Anh Dang. Design and Optimization for a New Compliant Planar Spring of Upper Limb Assistive Device Using Hybrid Approach of RSM–FEM and MOGA. *Arabian Journal for Science and Engineering*. 2019;44(9):7441–7456. Available from: <https://dx.doi.org/10.1007/s13369-019-03795-w>.
- 14) Jia J, Sun X. Structural Optimization Design of a Six-Degrees-of-Freedom Serial Robot with Integrated Topology and Dimensional Parameters. *Sensors*. 2023;23(16):1–20. Available from: <https://dx.doi.org/10.3390/s23167183>.
- 15) Chelladurai SJS, K KM, Ray AP, Upadhyaya M, Narasimharaj V, Gnanasekaran S. Optimization of process parameters using response surface methodology: A review. *Materials Today: Proceedings*. 2021;37(Part 2):1301–1304. Available from: <https://dx.doi.org/10.1016/j.matpr.2020.06.466>.
- 16) DOĞAN O, KALAY O, KARTAL E, KARPAT F. Optimum Design of Brake Pedal for Trucks Using Structural Optimization and Design of Experiment Techniques. *International Journal of Automotive Science and Technology*. 2020;4(4):272–280. Available from: <https://dx.doi.org/10.30939/ijastech..783552>.